CHEMISTRY OF MATERIALS

ARTICLE

pubs.acs.org/cm

Simple Route to Size-Tunable Degradable and Electroactive Nanoparticles from the Self-Assembly of Conducting Coil−Rod−Coil Triblock Copolymers

Baolin Guo, Anna Finne-Wistrand, and Ann-Christine Albertsson*

Department of Fibre and Polymer Technology, School of Chemical Science and Engineering, Royal Institute of Technology, SE-100 44, Stockholm, Sweden

ABSTRACT: A simple route to size-tunable nanoparticles from the self-assembly of degradable and electrically conductive coil−rod−coil triblock copolymers based on an aliphatic polyester and conducting species is presented. A series of coil−rod−coil triblock copolymers consisting of a middle aniline pentamer (AP) segment and two polycaprolactone (PCL) segments were easily synthesized by a combination of a ring-opening polymerization of CL initiated by an aniline dimer (AD) giving AD-PCL and an oxidative coupling reaction between the AD-PCL and p-phenylenediamine. This strategy avoids the multistep reaction used in previous work. The electroactivity of these copolymers was investigated by UV and cyclic voltammetry. The conductivity of the copolymers was dependent on the AP content and the conductivity mechanism of the triblock copolymers is discussed. Interestingly, these triblock copolymers can undergo self-assembly in selective solvent such as $CHCl_3$ as indicated by NMR and transmission electron microscope (TEM) observations. Dynamic light scattering (DLS) showed that the size of the nanoparticles was dependent on the molecular weight of the copolymers and on the oxidation state of the AP. The morphology of the nanoparticles was studied by TEM and SEM. These triblock copolymers and their size-tunable nanoparticles with degradability and electroactivity offer new possibilities in biomedical applications, such as controlled drug delivery, biosensors, and cardiovascular and neural tissue engineering.

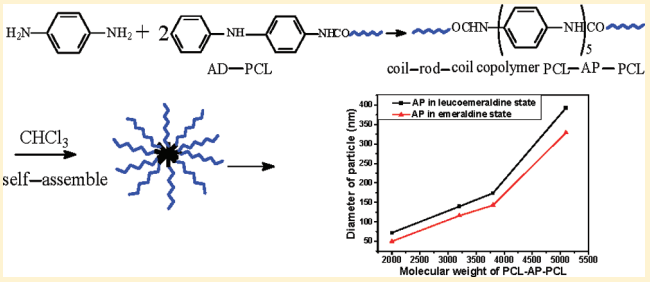

KEYWORDS: degradable and electroactive polymers, functionalization, conjugated polymers, amphiphilic, core−shell micelle

INTRODUCTION

Well-defined and functional supramolecular architectures from the self-assembly of block copolymers have a great potential in materials science, nanotechnology, and biomimetic chemistry.[1−3] Block copolymers, because of the physical incompatibility between the different covalently connected blocks undergo self-assembly in selective solvents into micelles with different morphologies, such as spherical, tubular, cylindrical, lamellae, vesicles, etc.[4,5] The self-assembly behavior and aggregates from diblock or triblock copolymers with flexible chains have been a hot topic during the past decade.[6−8] Recently, the self-assembly of rod−coil or coil−rod−coil block copolymers has attracted increasing interest[9−13] because or the functionality of the rigid-rod block and the assembly behavior different from that of the classical coil−coil amphiphilic diblock or triblock copolymers.

Biomaterials have been designed to induce a specific response at the molecular level.[14] Stimulus-responsive polymers controlled or tuned by external stimulation are being developed to meet the requirements of clinical treatment.[15−17] Electrically conducting polymers such as polyaniline and polypyrrole have been proven to tune the proliferation and differentiation of many different kinds of cells.[18−20] Aniline oligomers with well-defined structures, good solubility in most organic solvents, and excellent electroactivity similar to that of polyaniline have been widely used to prepare functional materials by our group and others.[21−26] Aniline oligomers with a rigid conformation are also good candidates for rod−coil and coil−rod−coil block copolymers that can assemble into functional nanomaterials.[27−29] For example, coil−rod−coil poly(ethylene glycol)-aniline pentamer-poly(ethylene glycol) (PEG) triblock[28] or rod−coil PEG-aniline tetramer diblock[29] copolymers were prepared by condensation polymerization between an aniline oligomer and PEG. These copolymers can assemble into micelles, and the particle size of the copolymers is dependent on the potential. The oligostyrene-oligoaniline-oligostyrene (St) triblock copolymer was synthesized,[27] and this copolymer self-assembled in tetrahydrofuran into aggregates with various morphologies such as spherical micelles and thin-layer vesicles. However, these copolymers were synthesized by a multistep reaction, and these micelles from copolymers with St or ether bonds in the main chain are not degradable.[30] The objective of the present work is to design a simple strategy for the preparation of degradable electroactive and size-tunable nanoparticles by the self-assembly of coil−rod−coil triblock

Received: June 22, 2011
Revised: July 28, 2011
Published: August 12, 2011

Scheme 1. Synthesis Routes of the Degradable and Conductive Triblock Copolymers

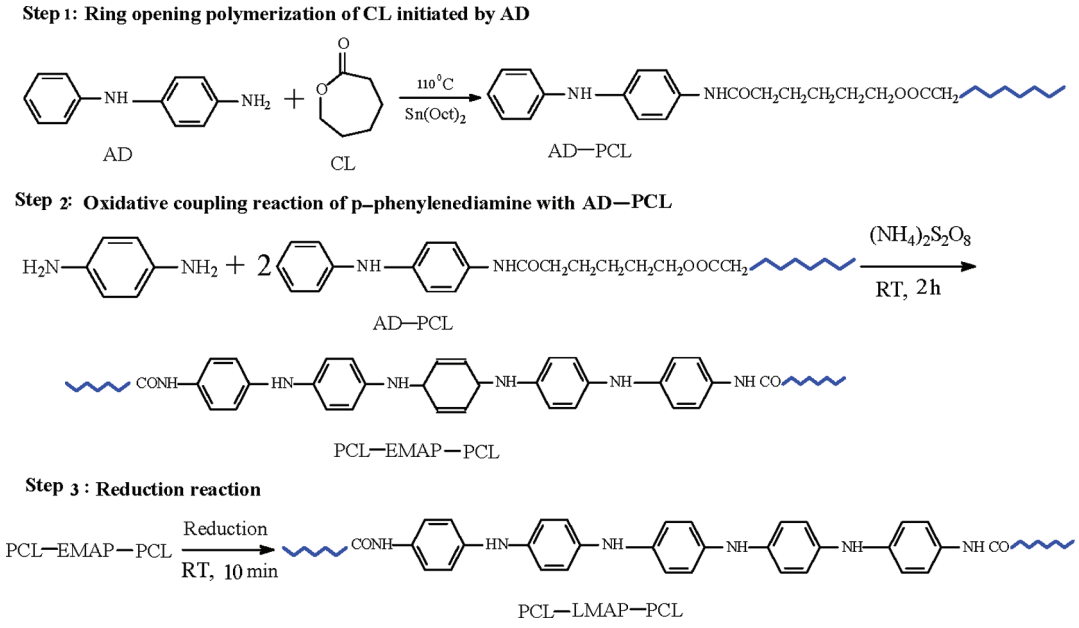

copolymers based on polyesters (such as polylactide, caprolactone, 1, 5-dioxepan-2-one, etc.) and aniline oligomers. We hypothesize (i) that we will obtain a degradable and electrically conductive coil−rod−coil triblock copolymer with a rigid aniline pentamer as middle block and two polyester flexible chains as side blocks through a simple synthesis by combining ring-opening polymerization and an oxidative coupling reaction, and thus avoid the multistep reaction used in previous work; (ii) that these coil−rod−coil triblock copolymers will assemble into core−shell micelles in a selective solvent such as chloroform (selective for PCL segment) due to their amphiphilic nature, and that we would obtain degradable electroactive nanoparticles by using an aliphatic polyester with a hydrolyzable ester bond in the main chain of the triblock copolymer, because aliphatic polyesters are biodegradable and the degradation rate is controllable;[31−33] and (iii) that we could easily tune the size of particles of these copolymers to meet a specific application by adjusting the molecular weight of the triblock copolymers and the oxidation state of the aniline oligomer. We here give an example of how to tune the size of the nanoparticles formed in the self-assembly of coil−rod−coil triblock copolymers composed of aniline pentamer (AP) and polycaprolactone (PCL). These size-tunable electroactive and degradable nanoparticles can be used in controlled drug delivery, biosensing, biodetection, and so on.

EXPERIMENTAL SECTION

Materials. Monomer ε-caprolactone (CL) from Aldrich was dried over CaH_2 for 48 h, and was then distilled under reduced pressure immediately before use. Stannous octoate, $Sn(Oct)_2$ (Aldrich) was dried over molecular sieves and stored in a glovebox (Mbraun MB 150B-G-I) purged with nitrogen. N-phenyl-1, 4-phenylenediamine (aniline dimer, AD), p-phenylenediamine, ammonium persulfate ($(NH_4)_2S_2O_8$), phenylhydrazine, ammonium hydroxide (NH_4OH), hydrochloric acid (HCl), dimethyl sulphoxide (DMSO), chloroform ($CHCl_3$), acetone, dimethyl formamide (DMF), hexane, and methanol were all purchased from Aldrich and used without further purification. The leucoemeraldine state of aniline pentamer (LMAP) was synthesized as described in our previous work.[23,34] ^{1}H NMR (400 MHz, DMSO-d_6): δ 12.09 (s, 2H, −COOH), 9.70 (s, 2H, −NHCO−), 7.63 (d, 2H, −NH−), 7.52 (s, 2H, −NH−), 7.38 (d, 4H, Ar−H), 6.85−6.94 (m, 16H, Ar−H).

Synthesis of AD-PCL. AD-PCL polymers with AD contents of 7.5, 10, 15, and 20% by weight in the polymers were synthesized as described in our previous paper[35] as shown in Scheme 1, the polymers being coded as AD7.5-PCL, AD10-PCL, AD15-PCL, and AD20-PCL, respectively. The yields of the AD-PCL polymers were between 90% and 94%. The ^{1}H NMR spectrum of AD15-PCL is shown in Figure 2A. AD15-PCL: ^{1}H NMR (400 MHz, DMSO-d_6): δ 9.70 (s, 1H, −CO−NH−), 8.00 (s, 1H, −NH−), 7.46 (d, 2H, Ar−H), 7.18 (t, 2H, Ar−H), 6.99 (m, 4H, Ar−H), 6.74 (m, 1H, Ar−H), 4.35 (t, 2H, −CO−CH_2−), 3.98 (m, 2H, −O−CH_2−), 2.27 (m, 2H, −CH_2−), 1.52 (m, 2H, −CH_2−), 1.28 (m, 2H, −CH_2−). AD15-PCL: ^{13}C NMR (100 MHz, DMSO-d_6): δ 172.76 (−COO−), 170.44 (−NHCO−), 144.17 (Ar−C), 138.50 (Ar−C), 132.36 (Ar−C), 129.08 (Ar−C), 120.30 (Ar−C), 118.82 (Ar−C), 117.87 (Ar−C), 114.71 (Ar−C), 63.61 (−CH_2O−), 60.64 (CO−CH_2−), δ = 33.37 (−CH_2−), 27.83 (−CH_2−), 24.87 (−CH_2−), 24.11 (−CH_2−).

Synthesis of Triblock PCL-AP-PCL Copolymers. The PCL-AP-PCL triblock copolymers were obtained by an oxidative coupling reaction between p-phenylenediamine and AD-PCL as shown in Scheme 1. The different feed ratios of the PCL-AP-PCL copolymer were listed in Table 1. Briefly, 500 mg AD15-PCL and 22 mg p-phenylenediamine were dissolved in a mixture of 6 mL DMF and 12 mL acetone, and 8 mL 1 mol/L HCl was then added. Four millilters $(NH_4)_2S_2O_8$ (92.9 mg) solution was added to the solution slowly in 20 min, and the mixture turned green. The mixture was allowed to react for 2 h at room temperature, and 100 mL of distilled water was then added. The mixture was filtered to collect the polymer, and the polymer was then washed with 200 mL of distilled water. The product was dedoped by 0.1 mol/L ammonium hydroxide for 10 min, and was then filtered to obtain the emeraldine state (EM) of the triblock copolymer PCL-EMAP15-PCL, which was reduced with phenylhydrazine to the leucoemeraldine state PCL-LMAP15-PCL. PCL-LMAP-PCL triblock copolymer was dissolved in $CHCl_3$ and precipitated in hexane/methanol

dx.doi.org/10.1021/cm201782v |Chem. Mater. 2011, 23, 4045–4055

(V:V = 95:5). This dissolution/precipitation process was repeated three times. The copolymers were finally dried in a vacuum oven for 72 h. The yields of the PCL-LMAP-PCL copolymers were 66−74%. The ^{1}H NMR spectra of PCL-LMAP15-PCL in DMSO-d_6 and $CDCl_3$ are shown in Figures 2B and 8a, respectively. PCL-LMAP15-PCL: ^{1}H NMR (400 MHz, DMSO-d_6): δ 9.61 (s, 2H, −CO−NH−), 7.63 (s, 2H, −NH−), 7.53 (s, 2H, −NH−), 7.37 (m, 4H, Ar−H), 6.99−6.84 (m, 16H, Ar−H), 4.35 (t, 2H, −CO−CH_2−), 3.98 (m, 2H, −O−CH_2), 2.27 (m, 2H, −CH_2−), 1.53 (m, 2H, −CH_2−), 1.28 (m, 2H, −CH_2−). PCL-LMAP15-PCL: ^{1}H NMR (400 MHz, $CDCl_3$): 4.05 (m, 2H, −CH_2−), 3.64 (m, 2H, −CH_2OH), 2.30 (m, 2H, −CH_2−), 1.64 (m, 2H, −CH_2−), 1.38 (m, 2H, −CH_2−).

Characterization. FT-IR spectra of the copolymers were recorded using a "Perkin Elmer Spectrum 2000′′-spectrometer (Perkin-Elmer Instrument, Inc.) in the range of 4000−600 cm^{-1}. Each spectrum was taken as the average of 16 scans at a resolution of 2 cm^{-1}.

^{1}H NMR and ^{13}C NMR spectra were obtained using a Bruker Avance 400 MHz NMR instrument, operating at 400.13 and 100.61 MHz, respectively. For the ^{1}H NMR and ^{13}C NMR measurements, 5−100 mg of the sample was dissolved in 1 mL DMSO-d_6 or $CDCl_3$. DMSO-d_6 and $CDCl_3$ were used as internal standards. The molecular weights of the AD-PCL and PCL-LMAP-PCL triblock copolymers shown in Table 2 were calculated by comparing the integral of the methylene −CH_2− group (δ 4.05 ppm) with that of the methylene protons next to the terminal hydroxyl group −CH_2OH (δ 3.64 ppm) as shown in Figure 8a.

Size exclusion chromatography (SEC) was used to determine the molecular weights (M_n) and molecular weight distributions (MWD) of the polymers. SEC was performed on a TDA Model 301 equipped with one or two GMH_{HR}-M columns with TSK-gel (Tosoh Biosep), a VE 5200 GPC Autosampler, a VE 1121 GPC solvent pump and a VE 5710 GPC degasser, which were from Viscotek Corp. Tetrahydrofuran was used as the mobile phase (flow rate 1.0 mL/min) at 35 °C. A conventional calibration was carried out using narrow linear polystyrene standards.

The UV−vis spectra of AD-PCL, PCL-LMAP-PCL, and PCL-EMAP-PCL copolymer solutions were recorded on a UV−vis spectrophotometer (UV-2401).

Table 1. Feed Ratio of the Degradable and Conductive Triblock Copolymers

sample code	*p*-phenylenediamine (mg)	ADx-PCL (mg)	$(NH_4)_2S_2O_8$ (mg)
PCL-AP7.5-PCL	11.0	500.0 (x = 7.5)	46.4
PCL-AP10-PCL	14.7	500.0 (x = 10)	62.1
PCL-AP15-PCL	22.0	500.0 (x = 15)	92.9
PCL-AP20-PCL	29.3	500.0 (x = 20)	123.7

Cyclic voltammetry (CV) of the PCL-LMAP-PCL polymers and LMAP was performed on a Potentiostat with a scan rate of 40 mV/s for all the samples. A platinum disk was used as working electrode (surface area 0.14 cm^2), a platinum-wire as auxiliary electrode, and an Ag/AgCl as reference electrode. Fifteen mg triblock copolymer PCL-LMAP-PCL or LMAP was dissolved in 6 mL DMSO, and was then doped with 0.2 mL 1 mol/L HCl. The mixture was purged with nitrogen for 10 min to remove oxygen prior to the CV measurements.

The conductivity of the PCL-EMAP-PCL with different EMAP contents was determined by a four-probe technique. Pellets of the triblock copolymers with a diameter of 2.0 cm and a thickness of about 0.05 cm were made in a compression mold at 40 °C.

Thermogravimetric Analysis (TGA) was performed on a Mettler Toledo TGA/SDTA851 TGA module and evaluated using STARe software. The test was performed at 10 °C min^{-1} with a nitrogen flow of 50 mL min^{-1} in the range from 50 to 800 °C.

Differential Scanning Calorimetry (DSC) measurements were carried out using a Mettler Toledo DSC820. The heating rate was 10 °C/min with a nitrogen flow of 50 mL/min. The samples were first heated to 100 °C and then cooled to −70 °C. The second scan was from −70 to 100 °C to obtain the heat of fusion. The crystallinity (X_c) was calculated from the second heating scan as: $X_c = \Delta H_f/\Delta H_f^0$, where ΔH_f is the enthalpy of fusion of the sample, and ΔH_f^0 is the enthalpy of fusion of a 100% crystalline PCL. The ΔH_f^0 of the PCL used in the calculations was 139.5 J/g.[36]

The morphology of the nanoparticles of the triblock copolymers was examined using a field emission scanning electron microscope (FE-SEM, S-4300, Hitachi, Japan). The samples were prepared by casting one drop of 0.5 wt % copolymer solution in $CHCl_3$ on a glass slide and allowing the $CHCl_3$ to evaporate for 2 h. Sample surfaces were then coated with a 5 nm thick gold layer before analysis.

Transmission electron microscopy (TEM) measurements were made on a Philips TECNAI 10 transmission electron microscope under an accelerating voltage of 80 KV. One drop of 0.5 wt % triblock copolymer solution in $CHCl_3$ was cast on a carbon-coated copper grid and the $CHCl_3$ was then evaporated for 2 h in air before the tests.

The particles size and size distribution (SD) of the aggregates from the triblock copolymers in $CHCl_3$ were determined by a Malvern Zetasizer Nano ZS with a He−Ne laser (633 nm) at 25 ± 0.1 °C. Scattered light was collected at a fixed angle of 90°. The 0.5 wt % triblock copolymer $CHCl_3$ solution was filtered through Millipore 0.45 μm filter prior to the test.

RESULTS AND DISCUSSION

Self-assembled π-conjugated nanostructures are of increasing interest due to their huge potential for functional nanomaterials.[37] One of the particularly interesting molecular architectures is that of oligoaniline, because it can easily be combined

Table 2. Properties of AD-PCL and PCL-LMAP-PCL Copolymers

sample code	M_n[a] (g/mol)	M_n[b] (g/mol)	MWD[b]	M_n theory (g/mol)	T_c (°C)	T_m (°C)	X_c
AD7.5-PCL	2500	2550	1.9	2450[c]	29.4	54.2	47.8
AD10-PCL	1900	2000	1.8	1850[c]	29.1	48.2	43.1
AD15-PCL	1400	1450	1.7	1250[c]	20.8	41.9	38.7
AD20-PCL	950	1150	1.7	950[c]	8.0	37.8	33.0
PCL-LMAP7.5-PCL	5700	5100	1.7	5100[d]	34.7	54.6	44.7
PCL-LMAP10-PCL	3900	3800	1.6	3900[d]	31.5	49.9	42.5
PCL-LMAP15-PCL	2750	3200	1.6	2900[d]	21.3	45.4	26.0
PCL-LMAP20-PCL	2100	2000	1.5	2000[d]	17.3	42.0	23.8

[a] Determined by ^{1}H NMR [b] Number average molecular weight and distribution determined by SEC [c] Theoretical number average molecular weight, M_n=[M]/[I]$_{co}$ × M_{CL} × Conversion [d] Theoretical number average molecular weight, M_n = 2M_n of AD-PCL + M_n of p-phenylenediamine

dx.doi.org/10.1021/cm201782v |Chem. Mater. 2011, 23, 4045–4055

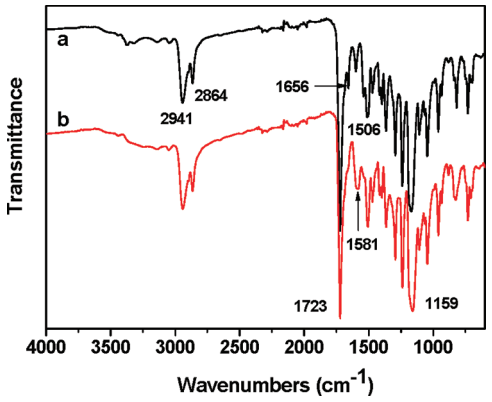

Figure 1. FT-IR Spectra of (a) PCL-LMAP15-PCL and (b) PCL-EMAP15-PCL.

by various chemical reactions to generate new nanostructured materials with special optical and electronic properties.[29,38,39] The chemical composition, the pH, the chain topology, and the molecular packing geometries have a great effect on the self-assembly of the π-conjugated block copolymers. The particle size of the aggregates is crucial for many applications, and tuning the particle size is a very challenging task. In this paper, we have easily synthesized the coil−rod−coil triblock copolymer PCL-AP-PCL in a two step reaction and, by changing the composition (molecular weights) of the copolymers and the oxidation state of the AP in the copolymer, we could tune the size of the particles from the self-assembly of the triblock copolymers in a simple and effective way.

Synthesis of Degradable and Conductive Triblock Copolymers. We developed a simple strategy for the synthesis of a degradable and electrically conductive coil−rod−coil triblock copolymer composed of a middle aniline pentamer block and two PCL side blocks in a two step reaction by combining ring-opening polymerization and an oxidative coupling reaction between one mole p-phenylenediamine and two moles AD-PCL polymers as shown in Scheme 1. This synthesis strategy is easy and precise, and the triblock copolymers obtained by this strategy have a well-defined structure and controlled molecular weight and properties. These coil−rod−coil triblock copolymers with an AP segment also have a higher conductivity than the diblock copolymers based on aniline tetramer described in our previous work.[35] By using AP as the center rod block, we overcome the nondegradability of polyaniline when polyaniline is used in a biomedical context where degradation is desired or even necessary, since the AP segment from the degradation of the triblock copolymer can be consumed by macrophages during the wound-healing response, and subsequently undergo renal clearance, avoiding the long-term adverse response.[40,41]

The FT-IR spectra of the PCL-LMAP15-PCL and PCL-EMAP15-PCL triblock copolymers are shown in Figure 1 as curves a and b, respectively. The absorption peaks at 1723 and 1159 cm^{-1} correspond to ester (−COO−) and ether (−C−O−C−) groups in the PCL segments. The peak at 1656 cm^{-1} is assigned to the absorption of the amide (−NHCO−) group which was formed during the ring-opening polymerization of caprolactone initiated by AD, indicating that ROP of CL did occur. The peaks at 1581 and 1506 cm^{-1} of PCL-EMAP15-PCL in curve b are ascribed to the characteristic absorption of the quinoid ring and benzene ring, respectively. The peak at 1581 cm^{-1} was absent in the PCL-LMAP15-PCL (curve a) indicating that the EMAP was successfully reduced into the LMAP segment.[23,42]

The well-defined structure of the triblock copolymers was further verified by the NMR spectrum shown in Figure 2. The peak of the amide group (−CONH−) in AD15-PCL appeared at 9.70 ppm indicating that the ring-opening polymerization of caprolactone initiated by AD had taken place. The peaks at 8.00 ppm and 6.74 ppm are assigned respectively to the secondary amine group (−NH−) of AD and the hydrogen in the benzene ring, as shown in Figure 2 (A). These two peaks are however absent in the spectrum of PCL-LMAP15-PCL copolymer, as shown in Figure 2B, but, two new peaks at about 7.63 and 7.53 ppm correspond to the −NH− groups in the LMAP segment, which confirmed that the oxidative coupling reaction between p-phenylenediamine and AD-PCL had occurred, and that the LMAP segment had been formed.

The molecular weights of the AD-PCL and PCL-LMAP-PCL copolymers were determined by SEC as shown in Figure 3. The SEC curves show only one symmetrical peak, and the PCL-LMAP-PCL triblock copolymers have less retention volume than the corresponding AD-PCL polymers. The retention volume of the PCL-LMAP-PCL copolymers increases with increasing AP content. The data for the molecular weights of the polymers are shown in Table 2. The molecular weight of the triblock copolymer is almost twice as high as that of the corresponding AD-PCL, indicating that the coupling reaction between *p*-phenylenediamine and AD-PCL occurred. The molecular weight distribution of the triblock copolymer was narrower than that of the corresponding AD-PCL copolymer. The molecular weights of the triblock copolymers obtained by SEC are consistent with those obtained by NMR, and are very close to the theoretical ones. This means that the oxidative coupling reaction between AD-PCL and p-phenylenediamine had a high reactivity and that the PCL segments were not degraded during the oxidative coupling reaction in acid solution. All these data confirmed that the PCL-LMAP-PCL triblock copolymers were successfully synthesized. These triblock copolymers with different molecular weights (different compositions of AP and PCL) can be used to tune the size of the self-assembled particles.

Electrochemical Properties of the Triblock Copolymers. Aniline pentamer has good electroactivity,[23,43] and the electroactivity is very important for the applications of conducting polymers in the biomedical filed.[18,19,44] The electrochemical properties of these triblock copolymers were characterized by UV absorption and cyclic voltammetry (CV). The UV absorption spectra in DMSO solution of AD20-PCL, PCL-LMAP20-PCL, PCL-EMAP20-PCL, and HCl-doped PCL-EMAP20-PCL are shown in Figure 4. The spectrum of AD20-PCL shows one peak at 304 nm corresponding to the absorption by the benzene ring. However, the PCL-EMAP20-PCL copolymer showed two absorption peaks at 316 and 605 nm, corresponding to the $\pi-\pi^*$ transition of the benzene ring and the excitonic transition from the benzene to the quinoid ring, respectively. This indicates that the AP was formed after the coupling reaction between p-phenylenediamine and AD20-PCL. The benzene ring absorption peak shifted to 316 nm in the PCL-EMAP-PCL copolymer since the EMAP segment has a much longer conjugated length than AD. The absorption of PCL-LMAP20-PCL showed only one peak at 322 nm corresponding to the $\pi-\pi^*$ transition of benzene ring, indicating that the reduction of PCL-EMAP-PCL by phenylhydrazine was complete. This result is consistent with

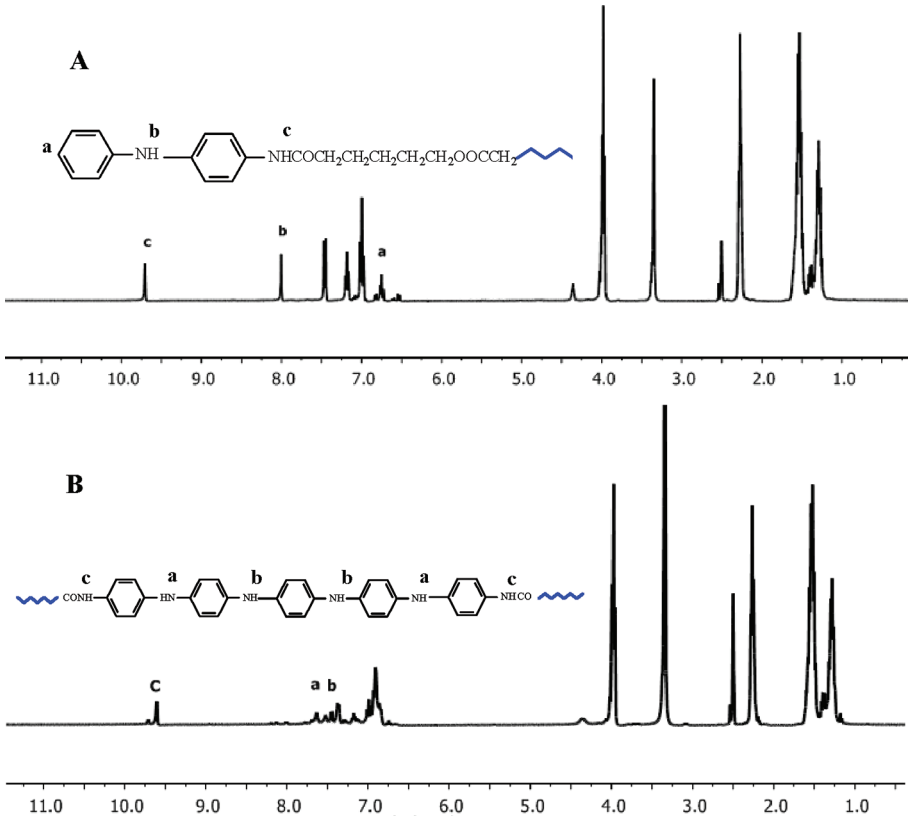

Figure 2. ^{1}H NMR spectra of (A) AD15-PCL and (B) PCL-LMAP15-PCL in DMSO-d_6.

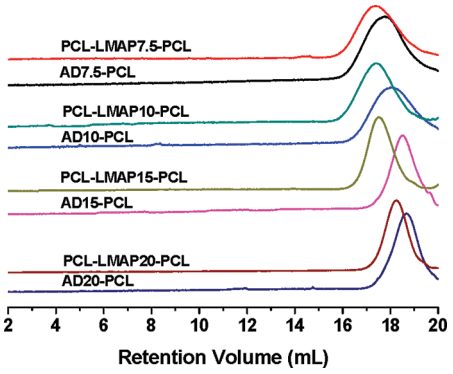

Figure 3. SEC curves of AD-PCL and their corresponding PCL-LMAP-PCL triblock copolymers.

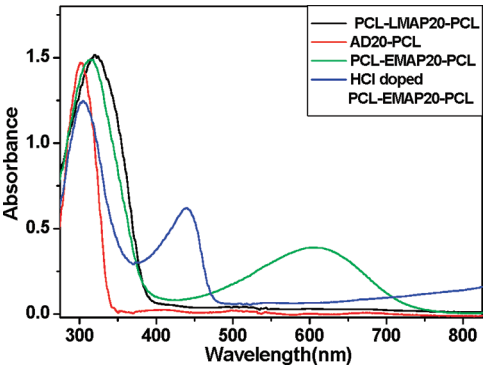

Figure 4. UV spectra of AD20-PCL, PCL-LMAP20-PCL, PCL-EMAP20-PCL, and HCl-doped PCL-EMAP20-PCL in DMSO solution.

the FT-IR spectrum shown in Figure 1. The benzene absorption of the HCl-doped PCL-EMAP20-PCL shifted to a lower wavelength at 305 nm, and the spectrum shows a new peak at 439 nm corresponding to the polaron absorption peak.[45] All these data confirm that the PCL-AP-PCL triblock copolymers were obtained.

Figure 5 shows that the benzene ring absorption peaks of PCL-LMAP7.5-PCL, PCL-LMAP10-PCL, PCL-LMAP15-PCL and PCL-LMAP20-PCL appeared at 306 nm, 310 nm, 314 nm, and 322 nm, respectively. The absorption of the copolymer solution shifted to a lower wavelength with increasing molecular weight of the copolymer. This phenomenon is similar to previous work of us and others.[35,42] The benzene absorption region shows the effective conjugation length of the system. The longer flexible PCL chains disturb more strongly the planar conformation of the LMAP segments, and this leads to a blue shift of the UV absorption. The absorption intensity of benzene ring of PCL-LMAP20-PCL, PCL-LMAP15-PCL, PCL-LMAP10-PCL, and PCL-LMAP7.5-PCL decreased in order, because the content of LMAP decreased accordingly in the copolymers.

Compared to the absorption peak in DMSO solution, the absorption peak of the PCL-LMAP20-PCL copolymers exhibited a blue shift in THF and $CHCl_3$ (Figure 5). This is ascribed to the polarity of the solvents. The lower polarity of THF and $CHCl_3$ results in a blue shift of the absorbance peak of the benzene ring.[24] The solubility of LMAP segment is relatively

dx.doi.org/10.1021/cm201782v |*Chem. Mater.* 2011, 23, 4045–4055

poor in THF and $CHCl_3$ although the solubility of the triblock copolymers in $CHCl_3$ is greatly improved due to the two long PCL segments. The PCL-LMAP-PCL triblock copolymers may self-assemble into micelles with LMAP as core, and PCL as shell in a selective solvent such as $CHCl_3$. This was verified by the ^1H NMR spectrum of the PCL-LMAP10-PCL triblock copolymer in $CDCl_3$, in which there is no peak corresponding to the LMAP segments, as shown in Figure 8a.

The chemical oxidation of the PCL-LMAP20-PCL in DMSO was studied by adding a trace amount of $(NH_4)_2S_2O_8$, and the UV spectra are shown in Figure 6. With increasing time, a new peak appeared at 605 nm corresponding to absorption by the quinoid ring together with a peak at 330 nm ascribed to a blue shift of the benzene ring in PCL-LMAP20-PCL. The intensity of the peak at 605 nm increased with time, and this peak then underwent a blue shift to 527 nm after reaching its maximum

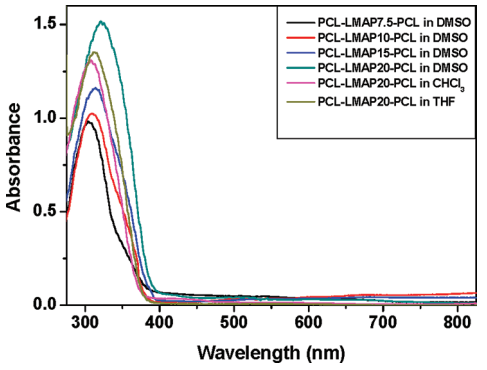

Figure 5. UV spectra of PCL-LMAP-PCL copolymers.

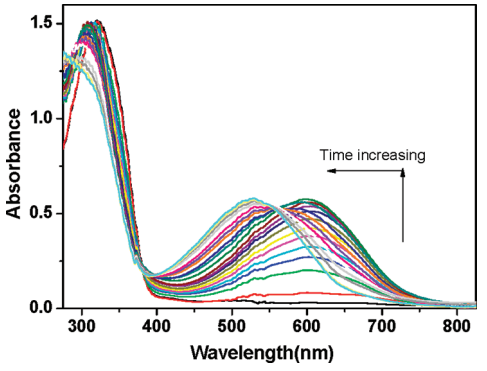

Figure 6. Oxidation of PCL-LMAP20-PCL in DMSO with a trace amount of $(NH_4)_2S_2O_8$.

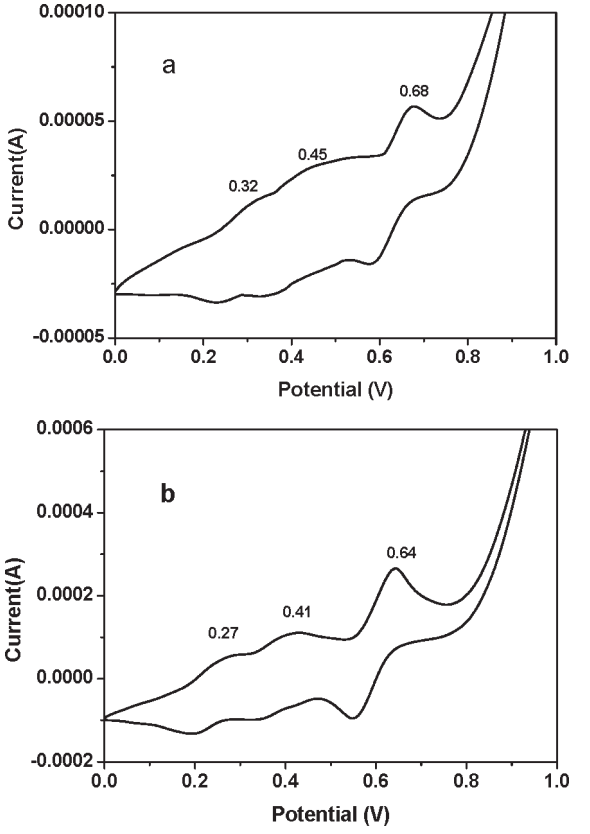

Figure 7. Cyclic voltammograms of (a) PCL-LMAP20-PCL and (b) LMAP in DMSO/HCl solution.

Scheme 2. Molecular Structure of Aniline Pentamer Segment in the Copolymer at Various Oxidation States

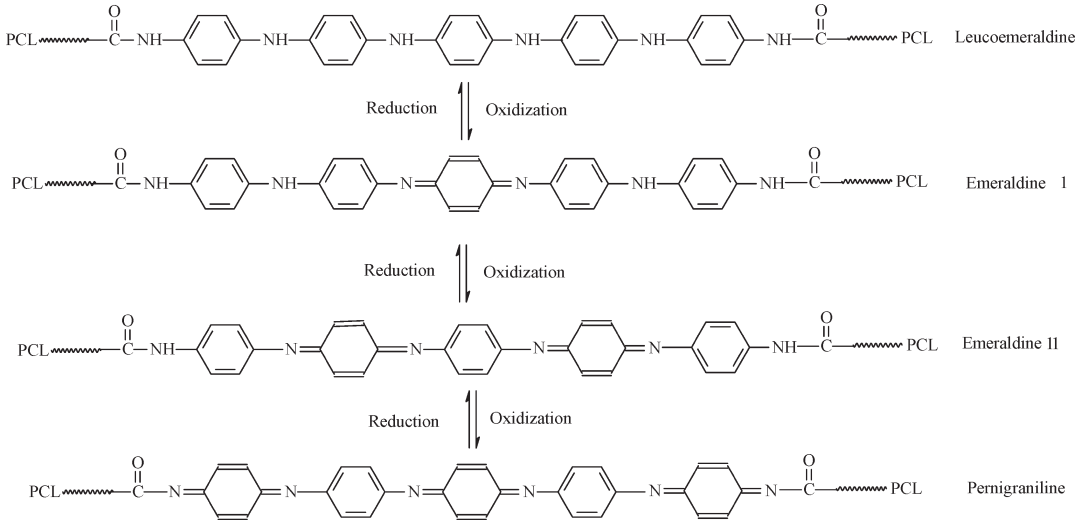

dx.doi.org/10.1021/cm201782v |*Chem. Mater.* 2011, 23, 4045–4055

Table 3. Conductivity of the Triblock Copolymers

sample code	conductivity (S/cm)	AP content % (theoretical)
PCL-EMAP7.5-PCL	5.58×10^{-7}	9 (9.4)
PCL-EMAP10-PCL	1.69×10^{-6}	12 (12.4)
PCL-EMAP15-PCL	3.74×10^{-6}	17 (18.2)
PCL-EMAP20-PCL	1.43×10^{-5}	23 (24.2)

intensity. This process can be explained by the three-step oxidation of the PCL-LMAP20-PCL copolymer shown in Scheme 2. At first, the PCL-LMAP20-PCL copolymer was in the leucoemeraldine state. It was then oxidized into the emeraldine I state with each AP unit having one quinoid ring, and then from the emeraldine I state to the emeraldine II state with each AP unit having two quinoid rings (Scheme 2). This leads to the appearance of a new absorption peak at 605 nm and the intensity of this peak increases with time. The copolymer was finally oxidized from the emeraldine II state to the pernigraniline state, and this caused the blue shift of the absorption peak from 605 to 527 nm. This oxidation of the PCL-LMAP20-PCL copolymer was confirmed by CV, as shown in Figure 7a. The CV of PCL-LMAP20-PCL copolymer exhibits three pair well-defined redox peaks. These peaks at 0.32 V, 0.45 V, and 0.68 V correspond respectively to the transition of the AP segment from the leucoemeraldine state to the emeraldine I state, from the emeraldine I state to the emeraldine II state, and finally from the emeraldine II state to the pernigraniline state (Scheme 2). The CV of the PCL-LMAP20-PCL is similar to that of the pure LMAP, as shown in Figure 7b. All these data indicate that the PCL-LMAP20-PCL was successfully synthesized, and that these triblock copolymers have good electroactivity.

Electrical Conductivity of PCL-EMAP-PCL Copolymers. Electrical conductivity of polyaniline can be achieved through interchain and intrachain transitions, and the conductivity can be 0.1−100 S/cm depending on the dopant and solvent employed.[45,46] The aniline oligomers such as AP have a much shorter chain length than polyaniline. The conductivity of the PCL-EMAP-PCL triblock copolymers is therefore much lower than that of polyaniline. The PCL-EMAP-PCL copolymers in $CHCl_3$ were doped with 1 mol/L HCl and the doped copolymers were then dried in a vacuum oven. The polymer was then compressed into pellets and the conductivity of their compressed pellets was tested by the four−probe technique. The data are listed in Table 3. The conductivity of the triblock copolymers is in the range from 1.43×10^{-5} to 5.58×10^{-7} S/cm with an EMAP content from 23% to 9% in the copolymers. This value of 1.43×10^{-5} S/cm is higher than that of tetramer-polycaprolactone (AT-PCL) reported in our previous work,[35] even though the AP content is much lower than that of AT in the AT-PCL copolymers. Although the conductivity value is much lower than that of AP films (10^{-2} S/cm), this conductivity value dependent on the EMAP content in the copolymer is sufficient for biomedical applications in the tuning of neural and cardiovascular cells, since the microcurrent in vivo is quite low.[47,48] The lower conductivity values of the triblock copolymers may be due to the incorporation of two long flexible nonconjugated PCL segments in the triblock copolymers. On the other hand, $CHCl_3$ is a good solvent for PCL segments and a poor solvent for EMAP segments, because of the different natures of PCL and EMAP. The PCL-EMAP-PCL triblock copolymer will therefore undergo self-assembly and form core−shell micelles in the $CHCl_3$ solution. The EMAP segments with a poor solubility in $CHCl_3$ aggregate together because of the strong interaction between the AP segments, and form a core of the particles. The PCL segments can easily dissolve in $CHCl_3$, and the PCL segments in an extended state thus form a shell of the particles, as shown in Scheme 3. With EMAP as core of the nanoparticles, the nonconductive PCL segments formed a continuous matrix in the compressed pellet. The electrons can easily transfer between different AP segments in the core where EMAP aggregates. However, a tunnel effect has to take place to achieve electrical conductivity between two neighboring EMAP cores. Consequently, the apparent conductivity of the PCL-EMAP-PCL triblock copolymer is quite low. We also found that the conductivity of the copolymers increases with increasing EMAP content. The molecular weight of the PCL segment in the triblock copolymers decreases with increasing EMAP content. The thickness of the shell of the nanoparticles thus decreases with increasing EMAP content in the copolymers, as shown in Scheme 3. The tunnel effect takes place more easily with a shorter distance between the two neighboring EMAP cores. Therefore, the higher EMAP content favors electron transfer and increases the electrical conductivity of the material.

Scheme 3. Proposed Self-Assembly of PCL-EMAP-PCL in $CHCl_3$

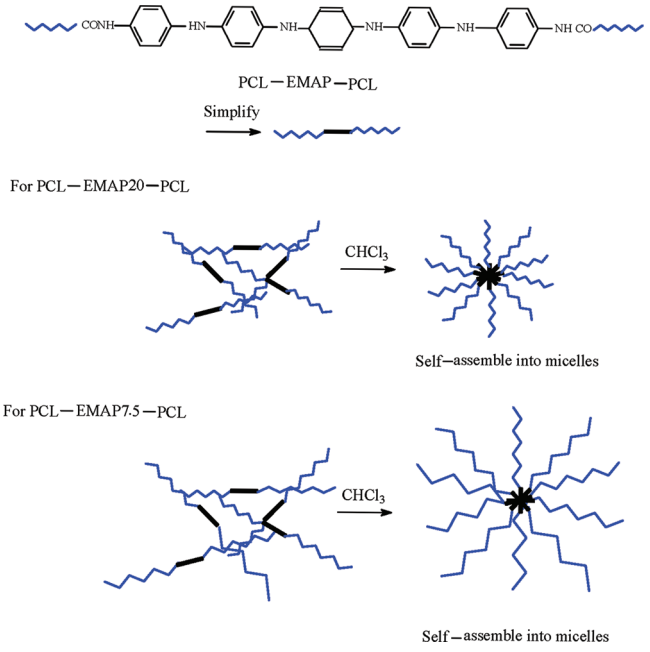

Self-Assembly of the Triblock Copolymers. Because of the amphiphilic nature of these triblock copolymers, PCL-LMAP-PCL and PCL-EMAP-PCL copolymers are expected to self-assemble into core−shell aggregates in a solvent selective for PCL (e.g., $CHCl_3$) with the two PCL segments stretching out as the shell and AP segment as core. This was demonstrated by the ^{1}H NMR spectrum of PCL-LMAP-PCL and PCL-EMAP-PCL copolymers in $CDCl_3$. Both the LMAP and EMAP signals in the ^{1}H NMR spectra disappeared, and the signals of the PCL segments were still present, as shown in Figure 8, indicating that these triblock copolymers formed aggregates with PCL as shell and AP segments as core where the external PCL shell shielded the signal of the internal AP core.[49,50] The DLS analysis of the

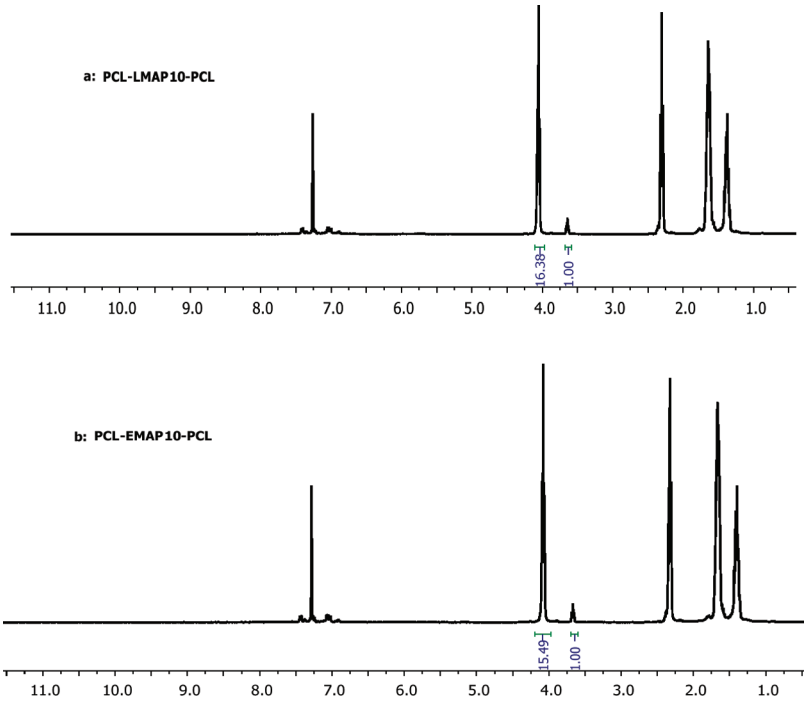

Figure 8. ^{1}H NMR spectra of (a) PCL-LMAP-PCL and (b) PCL-EMAP-PCL in $CDCl_3$.

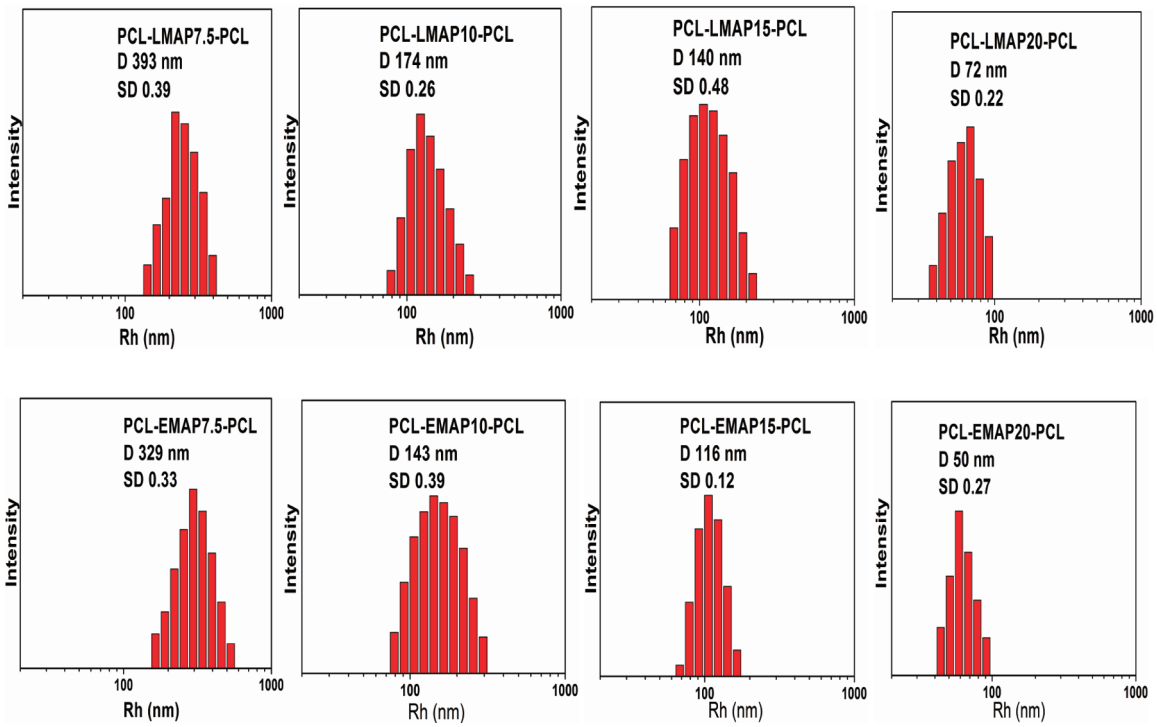

Figure 9. Size (D) and size distribution (SD) of the nanoparticles of the triblock copolymers determined by DLS.

0.5 wt % solution of the triblock copolymers in $CHCl_3$ also indicated that these triblock copolymers self-assembled into nanoparticles with a narrow distribution, as shown in Figure 9. The morphology of the nanoparticles was investigated by TEM, and the TEM image of the nanoparticles from copolymer PCL-EMAP10-PCL is shown as an example in Figure 10a. The particle of PCL-EMAP10-PCL showed a spherical morphology with a diameter of about 160 nm, which is consistent with the DLS results. These results for the PCL-EMAP10-PCL copolymers were confirmed by SEM as shown in Figure 10b, where the particles exhibit a spherical morphology and a diameter of about 180 nm.

As shown in Figure 9, the hydrodynamic diameters of these nanoparticles ranges from 393 to 50 nm increased with

dx.doi.org/10.1021/cm201782v |*Chem. Mater.* 2011, 23, 4045–4055

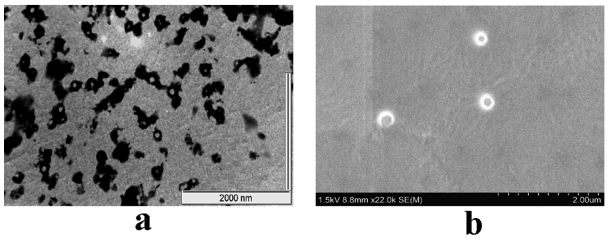

Figure 10. (a) TEM and (b) SEM images of the nanoparticles from PCL-EMAP10-PCL.

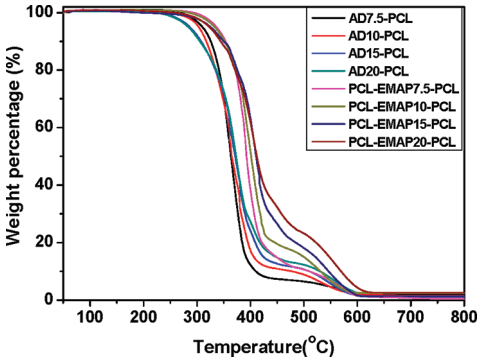

Figure 11. Thermal stability of AD-PCL and PCL-EMAP-PCL copolymers.

increasing molecular weight or decreasing AP content in these PCL-LMAP-PCL and PCL-EMAP-PCL triblock copolymers. This may be because the higher molecular weight of the copolymer is associated with a longer PCL chains, and the thickness of the shell of their aggregates would increase (Scheme 3). The aggregates thus have a larger diameter in $CHCl_3$ with increasing molecular weight of the triblock copolymers. Figure 9 also shows that the nanoparticles obtained from PCL-LMAP-PCL copolymer are larger than those of the corresponding PCL-EMAP-PCL copolymers. This is probably because, when PCL-LMAP-PCL is oxidized to PCL-EMAP-PCL state, the greater rigidity of the EMAP segment hinders chain rotation, and the free space in the core which is occupied by EMAP decreases, resulting in a decrease in conformation entropy of the EMAP copolymer compared to that of the LMAP copolymer. Consequently, the EMAP copolymers have a relatively higher interface curvature,[51] and the nanoparticles of PCL-EMAP-PCL are smaller than those of the corresponding PCL-LMAP-PCL copolymer. This result is consistent with previous report.[52] The size of the nanoparticles from these triblock copolymers was thus tuned by the molecular weight of the triblock copolymers and the oxidation state of the AP segments, and this offers a potential application in controlled drug delivery, biosensors, etc.

Thermal Properties of the Copolymers. The thermal properties of these polymers are also very important for their application, and they were studied by TGA and DSC. The TGA thermograms of the triblock copolymers are shown in Figure 11. The thermal degradation behavior of PCL-EMAP-PCL copolymers is similar to that of the AD-PCL polymers. In the case of the PCL-EMAP-PCL copolymers, the first obvious weight loss took place in the temperature range between 310 °C and 440−460 °C, attributed to the decomposition of the less

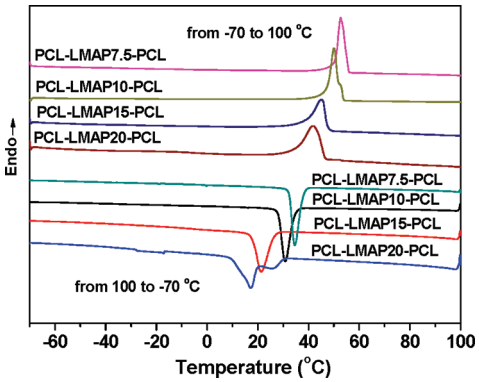

Figure 12. DSC curves of PCL-LMAP-PCL triblock copolymers.

thermally stable PCL segments. When the temperature was increased from 440−460 °C to 620 °C, there was a second evident weight loss of about 25−10 wt % copolymer, which corresponds to the degradation of the EMAP segment. In the case of the AD-PCL polymers, the thermal degradation occurs at a lower temperature, indicating that the PCL-EMAP-PCL copolymers have a greater thermal stability, presumably because the PCL-EMAP-PCL copolymer has a longer conjugated system and a higher EMAP content in the PCL-EMAP-PCL copolymer than that of AD in the AD-PCL polymers. The EMAP contents were calculated from the second degradation stage of the PCL-EMAP-PCL copolymers where the PCL segments were completely degraded. The data are shown in Table 3, and EMAP contents in the copolymers determined by TGA are very close to the theoretical values, which further confirmed that the PCL-EMAP-PCL copolymers were obtained. The PCL-LMAP-PCL copolymers exhibited a thermal degradation behavior similar to that of the PCL-EMAP-PCL copolymers. These data show that these triblock copolymers have a good thermal stability.

The crystallization temperature (T_c), melting temperature (T_m), and crystallinity (X_c) of the PCL-LMAP-PCL triblock copolymers were studied by DSC, and the DSC curves are shown in Figure 12. The T_c of the PCL-LMAP-PCL triblock copolymers decreases with increasing LMAP content, as shown in Table 2. This is because the rigid LMAP hinders the PCL segment from movement into the lattice. The triblock copolymers have a higher T_c than that of the corresponding AD-PCL polymers. This is different from our previous work,[35] where the aniline tetramer-polycaprolactone (AT-PCL) diblock copolymers had a lower T_c than the AD-PCL polymers. This may be because the PCL-LMAP-PCL copolymers have an AP content lower than that of AT in AT-PCL copolymers. The lower LMAP content in the triblock copolymer would disturb the crystallization of the copolymers less. Due to their higher crystallization ability, the triblock copolymers have a more perfect crystal, and thus a higher T_m than that of AD-PCL polymers (Table 2). On the other hand, the entanglements between the macromolecules of the PCL-LMAP-PCL triblock copolymer are much stronger than those of the corresponding AD-PCL polymers because of their higher molecular weight. This impedes the crystallization of the PCL-LMAP-PCL copolymer, and decreases their crystallinity. This results in a lower crystallinity of the PCL-LMAP-PCL triblock copolymer than that of the corresponding AD-PCL polymer (Table 2). Furthermore, the LMAP content increases with decreasing molecular weight of the PCL-LMAP-PCL copolymer

dx.doi.org/10.1021/cm201782v |*Chem. Mater.* 2011, 23, 4045–4055

and the rigid LMAP segments disturb the crystallization of the triblock copolymer. Thus, the crystallinity of the triblock copolymer decreases with increasing LMAP content.

By using degradable and electroactive coil−rod−coil triblock copolymers based on PCL and aniline pentamer as an example, we have shown how to tune the nanoparticles from the self-assembly of these copolymers in an easy and effective way. Because of the facile synthesis of the triblock copolymers and the special properties of these nanoparticles, this strategy will generate a library of size-tunable, degradable and electroactive nanoparticles with different degradation properties, thermal properties, and hydrophilicities based on an aniline pentamer and polyesters such as polylactide, polycaprolactone, poly (1, 5-dioxepan-2-one), poly(trimethylene carbonate), etc.

CONCLUSIONS

Size-tunable nanoparticles with hydrolyzable ester bonds and electroactivity from the self-assembly of electrically conductive coil−rod−coil triblock copolymers based on polycaprolactone and aniline pentamer (AP) have been successfully prepared by a simple strategy. A library of triblock copolymers with degradability and electroactivity has been easily synthesized by the combination of ring-opening polymerization and the oxidative coupling reaction, as demonstrated by FT-IR, NMR, and SEC. These triblock copolymers exhibit good electroactivity as indicated by CV and UV. The electrical conductivity of the triblock copolymers was between 5.58×10^{-7} and 1.43×10^{-5} S/cm, and this was achieved by the combination of the electron transfer inside the EMAP core and a tunnel effect between the neighboring EMAP cores. These triblock copolymers underwent self-assembly in $CHCl_3$ and formed core−shell spherical nanoparticles with aniline pentamer as core and PCL as shell, as indicated by NMR. The particle size between 393 and 50 nm increased with increasing molecular weight of the triblock copolymers, and the particle size of the triblock copolymers with the leucoemeraldine state of AP was greater than that of the corresponding copolymer with the emeraldine state of AP. These degradable and electroactive nanoparticles, size-tunable by the molecular weight and oxidation state of AP in the copolymers have a great potential in the biomedical field.

AUTHOR INFORMATION

Corresponding Author

*Tel.:+46-8-790 8274. Fax: +46-8-20 84 77. E-mail: aila@polymer.kth.se.

ACKNOWLEDGMENT

The authors thank the China Scholarship Council (CSC) and The Royal Institute of Technology (KTH) for financial support for this work.

REFERENCES

(1) Lee, M.; Cho, B. K.; Zin, W. C. *Chem. Rev.* **2001**, *101*, 3869–3892.
(2) Mao, Z. W.; Xu, H. L.; Wang, D. Y. *Adv. Funct. Mater.* **2010**, *20*, 1053–1074.
(3) Cayre, O. J.; Chagneux, N.; Biggs, S. *Soft Matter* **2011**, *7*, 2211–2234.
(4) Zhang, L. F.; Eisenberg, A. *Science* **1995**, *268*, 1728–1731.
(5) Darling, S. B. *Prog. Polym. Sci.* **2007**, *32*, 1152–1204.
(6) Jain, S.; Bates, F. S. *Science* **2003**, *300*, 460–464.
(7) Abetz, V.; Simon, P. F. W. Phase behaviour and morphologies of block copolymers. In *Advances in Polymer Science*; Springer-Verlag: Berlin, 2005; Vol. 189, pp 125−212.
(8) Shenhar, R.; Norsten, T. B.; Rotello, V. M. *Adv. Mater.* **2005**, *17*, 657–669.
(9) Stupp, S. I.; LeBonheur, V.; Walker, K.; Li, L. S.; Huggins, K. E.; Keser, M.; Amstutz, A. *Science* **1997**, *276*, 384–389.
(10) He, P. T.; Li, X. J.; Deng, M. G.; Chen, T.; Liang, H. J. *Soft Matter* **2010**, *6*, 1539–1546.
(11) Wang, H. B.; Wang, H. H.; Urban, V. S.; Littrell, K. C.; Thiyagarajan, P.; Yu, L. P. *J. Am. Chem. Soc.* **2000**, *122*, 6855–6861.
(12) Tian, L. R.; Zhong, K. L.; Liu, Y. J.; Huang, Z. G.; Jin, L. Y.; Hirst, L. S. *Soft Matter* **2010**, *6*, 5993–5998.
(13) Jin, L. Y.; Bae, J.; Ryu, J. H.; Lee, M. *Angew. Chem., Int. Ed.* **2006**, *45*, 650–653.
(14) Hench, L. L.; Polak, J. M. *Science* **2002**, *295*, 1014.
(15) Alarcon, C. D. H.; Pennadam, S.; Alexander, C. *Chem. Soc. Rev.* **2005**, *34*, 276–285.
(16) Tokarev, I.; Minko, S. *Soft Matter* **2009**, *5*, 511–524.
(17) Costa, R. R.; Custodio, C. A.; Testero, A. M.; Arias, F. J.; Rodriguez-Cabello, J. C.; Alves, N. M.; Mano, J. F. *Adv. Funct. Mater.* **2009**, *19*, 3210–3218.
(18) Schmidt, C. E.; Shastri, V. R.; Vacanti, J. P.; Langer, R. *Proc. Nat. Acad. Sci. U.S.A.* **1997**, *94*, 8948–8953.
(19) Gomez, N.; Lee, J. Y.; Nickels, J. D.; Schmidt, C. E. *Adv. Funct. Mater.* **2007**, *17*, 1645–1653.
(20) Guimard, N. K.; Gomez, N.; Schmidt, C. E. *Prog. Polym. Sci.* **2007**, *32*, 876–921.
(21) Buga, K.; Majkowska, A.; Pokrop, R.; Zagorska, M.; Djurado, D.; Pron, A.; Oddou, J. L.; Lefrant, S. *Chem. Mater.* **2005**, *17*, 5754–5762.
(22) Weng, C. J.; Chang, C. H.; Peng, C. W.; Chen, S. W.; Yeh, J. M.; Hsu, C. L.; Wei, Y. *Chem. Mater.* **2011**, *23*, 2075–2083.
(23) Guo, B. L.; Finne-Wistrand, A.; Albertsson, A. C. *Macromolecules* **2010**, *43*, 4472–4480.
(24) Guo, B. L.; Finne-Wistrand, A.; Albertsson, A. C. *Biomacromolecules* **2010**, *11*, 855–863.
(25) Guo, B. L.; Finne-Wistrand, A.; Albertsson, A. C. *Chem. Mater.* **2011**, *23*, 1254–1262.
(26) Guo, B. L.; Finne-Wistrand, A.; Albertsson, A. C. *Biomacromolecules* **2011**, *12*, 2601–2609.
(27) Wang, H. F.; Han, Y. C. *Macromol. Rapid Commun.* **2009**, *30*, 521–527.
(28) Hu, J.; Zhuang, X. L.; Huang, L. H.; Lang, L.; Chen, X. S.; Wei, Y.; Jing, X. B. *Langmuir* **2008**, *24*, 13376–13382.
(29) Kim, H.; Jeong, S. M.; Park, J. W. *J. Am. Chem. Soc.* **2011**, *133*, 5206–5209.
(30) Knop, K.; Hoogenboom, R.; Fischer, D.; Schubert, U. S. *Angew. Chem.-Int. Edit.* **2010**, *49*, 6288–6308.
(31) Hakkarainen, M.; Hoglund, A.; Odelius, K.; Albertsson, A. C. *J. Am. Chem. Soc.* **2007**, *129*, 6308–6312.
(32) Hoglund, A.; Odelius, K.; Hakkarainen, M.; Albertsson, A. C. *Biomacromolecules* **2007**, *8*, 2025–2032.
(33) Hakkarainen, M.; Adamus, G.; Hoglund, A.; Kowalczuk, M.; Albertsson, A. C. *Macromolecules* **2008**, *41*, 3547–3554.
(34) Guo, B. L.; Finne-Wistrand, A.; Albertsson, A. C. *J. Polym. Sci., Part A: Polym. Chem.* **2011**, *49*, 2097–2105.
(35) Guo, B. L.; Finne-Wistrand, A.; Albertsson, A. C. *Macromolecules* **2011**, *44*, 5227–5236.
(36) Malberg, S.; Plikk, P.; Finne-Wistrand, A.; Albertsson, A. C. *Chem. Mater.* **2010**, *22*, 3009–3014.
(37) Stejskal, J.; Sapurina, I.; Trchova, M. *Prog. Polym. Sci.* **2010**, *35*, 1420–1481.
(38) Kim, H.; Park, J. W. *J. Mater. Chem.* **2010**, *20*, 1186–1191.
(39) Yang, Z. F.; Wang, X. T.; Yang, Y. K.; Liao, Y. G.; Wei, Y.; Xie, X. L. *Langmuir* **2010**, *26*, 9386–9392.
(40) Rivers, T. J.; Hudson, T. W.; Schmidt, C. E. *Adv. Funct. Mater.* **2002**, *12*, 33–37.

(41) Zelikin, A. N.; Lynn, D. M.; Farhadi, J.; Martin, I.; Shastri, V.; Langer, R. *Angew. Chem., Int. Ed.* **2002**, *41*, 141–144.
(42) Huang, L. H.; Hu, J.; Lang, L.; Wang, X.; Zhang, P. B.; Jing, X. B.; Wang, X. H.; Chen, X. S.; Lelkes, P. I.; MacDiarmid, A. G.; Wei, Y. *Biomaterials* **2007**, *28*, 1741–1751.
(43) Hung, W. I.; Hung, C. B.; Chang, Y. H.; Dai, J. K.; Li, Y.; He, H.; Chen, S. W.; Huang, T. C.; Wei, Y.; Jia, X. R.; Yeh, J. M. *J. Mater. Chem.* **2011**, *21*, 4581–4587.
(44) Kim, D. H.; Richardson-Burns, S. M.; Hendricks, J. L.; Sequera, C.; Martin, D. C. *Adv. Funct. Mater.* **2007**, *17*, 79–86.
(45) Xia, Y. N.; Wiesinger, J. M.; Macdiarmid, A. G.; Epstein, A. J. *Chem. Mater.* **1995**, *7*, 443–445.
(46) Bhadra, S.; Khastgir, D.; Singha, N. K.; Lee, J. H. *Prog. Polym. Sci.* **2009**, *34*, 783–810.
(47) Huang, L. H.; Zhuang, X. L.; Hu, J.; Lang, L.; Zhang, P. B.; Wang, Y. S.; Chen, X. S.; Wei, Y.; Jing, X. B. *Biomacromolecules* **2008**, *9*, 850–858.
(48) Niple, J. C.; Daigle, J. P.; Zaffanella, L. E.; Sullivan, T.; Kavet, R. *Bioelectromagnetics* **2004**, *25*, 369–373.
(49) Li, W.; Li, J. F.; Gao, J.; Li, B. H.; Xia, Y.; Meng, Y. C.; Yu, Y. S.; Chen, H. W.; Dai, J. X.; Wang, H.; Guo, Y. J. *Biomaterials* **2011**, *32*, 3832–3844.
(50) Sun, T. M.; Du, J. Z.; Yan, L. F.; Mao, H. Q.; Wang, J. *Biomaterials* **2008**, *29*, 4348–4355.
(51) Wang, H. F.; Guo, P.; Han, Y. C. *Macromol. Rapid Commun.* **2006**, *27*, 63–68.
(52) Huang, L. H.; Hu, J.; Lang, L.; Chen, X. S.; Wei, Y.; Jing, X. B. *Macromol. Rapid Commun.* **2007**, *28*, 1559–1566.